

Numerical Modeling of Submarine Mass-Movement Generated Waves Using RANS Model

D. YUK and S. YIM

Oregon State University, Department of Civil Engineering, Corvallis, OR, USA

P. L.-F. LIU

Cornell University, School of Civil and Environmental Engineering, Ithaca, NY, USA

Abstract

In this paper a numerical model for predicting waves generated by nearshore submarine mass-movements is described. The model is based on the Reynolds Averaged Navier-Stokes (RANS) equations with the $k - \epsilon$ turbulence model. The volume of fluid (VOF) method is employed to track the free surface. The submarine mass movement is prescribed. Numerical results obtained from the present model are validated with laboratory experiments and analytical solutions. Very good agreements are observed.

Keyword: Submarine mass movement, numerical model, turbulence, breaking waves

1 Introduction

Motivated by the needs for preservation of human lives and coastal infrastructures, and for the deployment and operation of special structural and mechanical systems in coastal areas, the study of nearshore wave motions and wave-structure interaction has been of interest to coastal scientists and engineers for many years.

Coastal wave generation due to submarine mass movement is a complex process. While the length-scale of a submarine mass movement is usually smaller than that of a seafloor displacement created by a fault rupture, the time-scale is usually longer. Therefore, the concept of "initial free surface displacement" in the wave generation region becomes a critical issue. Hence the evolution of the free surface displacement in the source region of mass movement needs to be modeled entirely. Furthermore, the characteristics of a submarine mass movement, including the soil properties, volume and area of the mass movement, also require a post-event bathymetry survey.

Several numerical models have been developed to describe the waves generated by submerged or aerial mass movements. With the common assumption that the geometry and the movement of the mass movement can be prescribed, these models adopt various additional approximations in hydrodynamics. For instance, Lynett & Liu (2002) presented a model based on the depth-integrated nonlinear wave equations, which include the frequency dispersion effects. Therefore, their model can simulate relatively short waves that might be generated by a submarine mass movement. Grilli & Watts (1999) adopted a Boundary Integral Equation Method, based on the potential flow theory, and developed a fully nonlinear model for mass movement-generated waves. However, the approach does not allow wave breaking, which could be important in the vicinity of the generation region as well as the runup region. The depth-averaged model suffers the same drawback as the BIEM model in terms of the lack of capability of modeling breaking waves, however, it is much more computationally efficient for it has reduced the 3D problem to a 2D problem in the

horizontal space. Heinrich (1992) modified the NASA-VOF2D model, which is a 2D (vertical plane) nonlinear free surface model based on the Navier-Stokes equations, to study the generation, propagation and runup of tsunamis created by landslides. The effects of turbulence are not considered. Heinrich compared his numerical results for both submarine and aerial mass movements with his own experiments. The agreement is reasonable, except in the regions where breaking induced turbulence is important.

In recent years, significant advancement in modeling the wave breaking process and the interactions between breaking waves and coastal structures has been made. For example, COBRAS (Cornell Breaking waves and Structures model) is based on the Reynolds Averaged Navier-Stokes (RANS) equations with a $k - \varepsilon$ turbulence closure model. While a nonlinear Reynolds stress model is employed to allow anisotropic turbulence, the Volume of Fluid (VOF) method is used to track the free surface movements. COBRAS has been verified by comparing numerical results with experimental data for runup and rundown of breaking waves on a uniform beach (Lin & Liu 1998 a, b, Lin *et al.* 1999). It has wave-structure interactions capability (Hsu *et al.* 2002) with rigid, stationary, fully submerged or surface piercing structures.

The primary goal of this paper is to modify COBRAS to allow time-dependent solid boundaries such that mass movement-created waves can be simulated. Since COBRAS is capable of calculating turbulence, the modified model will be able to simulate breaking waves and runup. In this paper, we shall first present briefly the theoretical background of COBRAS and discuss the necessary modification to simulate the mass movement. 2D numerical results are then compared with experimental data. Some discussions on the future extensions are given at the end of the paper.

2 Description of the model

In this section the mathematical formulation and the associated numerical algorithm of COBRAS are discussed briefly. More detailed discussions can be found in Lin and Liu (1998 a, b). The model is based on the Reynolds Averaged Navier-Stokes (RANS) equations. For a turbulent flow, the velocity field and pressure field can be decomposed into two parts: the mean (ensemble average) velocity and pressure $\langle u_i \rangle$ and $\langle p \rangle$, and the turbulent velocity and the pressure u'_i and p' . Thus, $u_i = \langle u_i \rangle + u'_i$ and $p = \langle p \rangle + p'$ in which $i = 1, 2, 3$ for a three-dimensional flow. If the fluid is assumed incompressible, the mean flow field is governed by the Reynolds Averaged Navier-Stokes equations:

$$\frac{\partial \langle u_i \rangle}{\partial x_i} = 0, \quad (1)$$

$$\frac{\partial \langle u_i \rangle}{\partial t} + \langle u_j \rangle \frac{\partial \langle u_i \rangle}{\partial x_j} = -\frac{1}{\rho} \frac{\partial \langle p \rangle}{\partial x_i} + g_i + \frac{1}{\rho} \frac{\partial \langle \tau_{ij} \rangle}{\partial x_j} - \frac{\partial \langle u'_i u'_j \rangle}{\partial x_j}, \quad (2)$$

in which ρ is the density of the fluid, g_i the i -th component of the gravitational acceleration, and mean molecular stress tensor $\langle \tau_{ij} \rangle = 2\mu \langle \sigma_{ij} \rangle$ with μ being the

molecular viscosity and $\langle \sigma_{ij} \rangle$, the rate of strain tensor of the mean flow. In the momentum equation (2), the influence of the turbulent fluctuations on the mean flow field is represented by the Reynolds stress tensor $-\rho \langle u'_i u'_j \rangle$. Many second-order turbulence closure models have been developed for different applications. In the present model, the Reynolds stress is expressed by a nonlinear algebraic stress model:

$$\rho \langle u'_i u'_j \rangle = \frac{2}{3} \rho k \delta_{ij} - C_d \frac{k^2}{\varepsilon} \left(\frac{\partial \langle u_i \rangle}{\partial x_j} + \frac{\partial \langle u_j \rangle}{\partial x_i} \right) - \rho \frac{k^3}{\varepsilon^2} \left[C_1 \left(\frac{\partial \langle u_i \rangle}{\partial x_l} \frac{\partial \langle u_l \rangle}{\partial x_j} + \frac{\partial \langle u_j \rangle}{\partial x_l} \frac{\partial \langle u_l \rangle}{\partial x_i} \right) + \frac{2}{3} \frac{\partial \langle u_l \rangle}{\partial x_k} \frac{\partial \langle u_k \rangle}{\partial x_l} \delta_{ij} \right] + C_2 \left(\frac{\partial \langle u_i \rangle}{\partial x_k} \frac{\partial \langle u_j \rangle}{\partial x_k} - \frac{1}{3} \frac{\partial \langle u_l \rangle}{\partial x_k} \frac{\partial \langle u_l \rangle}{\partial x_k} \delta_{ij} \right) + C_3 \left(\frac{\partial \langle u_k \rangle}{\partial x_i} \frac{\partial \langle u_k \rangle}{\partial x_j} - \frac{1}{3} \frac{\partial \langle u_l \rangle}{\partial x_k} \frac{\partial \langle u_l \rangle}{\partial x_k} \delta_{ij} \right) \quad (3)$$

in which C_d, C_1, C_2 and C_3 are empirical coefficients, δ_{ij} the Kronecker delta, $k = \langle u'_i u'_i \rangle / 2$ the turbulent kinetic energy, and $\varepsilon = \nu \langle (\partial u'_i / \partial x_j)^2 \rangle$ the dissipation rate of turbulent kinetic energy, where $\nu = \mu / \rho$ is the molecular kinematic viscosity. It is noted that for the conventional eddy viscosity model $C_1 = C_2 = C_3 = 0$ in (3) and the eddy viscosity is then expressed as $\nu_t = C_d k^2 / \varepsilon$. Compared with the conventional eddy viscosity model, the nonlinear Reynolds stress model (3) can be applied to general anisotropic turbulent flows.

The governing equations for k and ε are modeled as (Lin and Liu, 1998 a, b),

$$\frac{\partial k}{\partial t} + \langle u_j \rangle \frac{\partial k}{\partial x_j} = \frac{\partial}{\partial x_j} \left[\left(\frac{\nu_t}{\sigma_k} + \nu \right) \frac{\partial k}{\partial x_j} \right] - \langle u'_i u'_j \rangle \frac{\partial \langle u_i \rangle}{\partial x_j} - \varepsilon, \quad (4)$$

$$\frac{\partial \varepsilon}{\partial t} + \langle u_j \rangle \frac{\partial \varepsilon}{\partial x_j} = \frac{\partial}{\partial x_j} \left[\left(\frac{\nu_t}{\sigma_\varepsilon} + \nu \right) \frac{\partial \varepsilon}{\partial x_j} \right] + C_{1\varepsilon} \frac{\varepsilon}{k} \nu_t \left(\frac{\partial \langle u_i \rangle}{\partial x_j} + \frac{\partial \langle u_j \rangle}{\partial x_i} \right) \frac{\partial \langle u_i \rangle}{\partial x_j} - C_{2\varepsilon} \frac{\varepsilon^2}{k}, \quad (5)$$

in which $\sigma_k, \sigma_\varepsilon, C_{1\varepsilon}$ and $C_{2\varepsilon}$ are empirical coefficients. The coefficients in equation (3) to (5) have been determined by performing many simple experiments and enforcing the

physical realizability; the recommended values for these coefficients can be found in Lin and Liu (1998 a, b).

Appropriate boundary conditions need to be specified. For the mean flow field, both the no-slip and the free-slip boundary condition can be imposed on the solid boundary. Along the mass surface, the velocity of the moving boundary is prescribed. The zero-stress condition is required on the mean free surface by neglecting the effect of airflow. For the turbulent field, near the solid boundary, the log-law distribution of mean tangential velocity in the turbulent boundary layer is applied so that the values of k and ε can be expressed as functions of distance from the boundary and the mean tangential velocity outside of the viscous sub-layer. On the free surface, the zero-gradient boundary conditions are imposed for both k and ε , *i.e.*, $\partial k / \partial n = \partial \varepsilon / \partial n = 0$. A low level of k for the initial and inflow boundary conditions is assumed.

In the numerical model, the RANS equations are solved by the finite difference two-step projection method. The forward time difference method is used to discretize the time derivative. The convection terms are discretized by the combination of central difference method and upwind method. The central difference method is employed to discretize the pressure gradient terms and stress gradient terms. The VOF method is used to track the free surface. The transport equations for k and ε are solved with the similar method used in solving the momentum equations (Lin and Liu 1998a,b).

3 Numerical Results and Discussions

To validate the numerical model, numerical simulations of several laboratory experiments have been carried out, including waves generated by vertical bottom movements (Hammack, 1973) and by a sliding triangular block on a uniform beach (Heinrich, 1992). In Hammack's experiments waves do not break in the generation region and the present numerical results agree with Hammack's data very well. In this paper we shall focus our discussion on Heinrich's experiments in which the generated waves break.

The computational domain is 12 m in x-direction and 2 m in y-direction. A variable grid size system is used in the x-direction with minimum grid size of 0.01 m and a fixed grid size of 0.01 m is employed in y-direction. To satisfy all stability conditions and restrictions of the incorporated methods, a fixed time step of 5×10^{-4} s is used. Numerical results in generation (*i.e.*, near moving mass) and propagation regions are compared with experimental data are shown in Figure 1 and 2. The submarine mass movement is modeled by a triangular shaped moving boundary that is initially located 0.01m below the free surface. The displacement time history measured from experiment is used to move the triangular mass. Since the grid size is not small enough to resolve boundary layer, the free-slip boundary condition is applied on all the solid boundaries including sliding body, slopes, and channel bottom. As shown in Figures 1 and 2, wave profiles in the generation region and the propagation region are in good agreement with experimental data. However, some deviations are observed in wave profile at $t = 1.5$ s when the reflected wave starts to break. It is surmised that the disagreement in wave profile is caused by the random nature of turbulence near wave breaking.

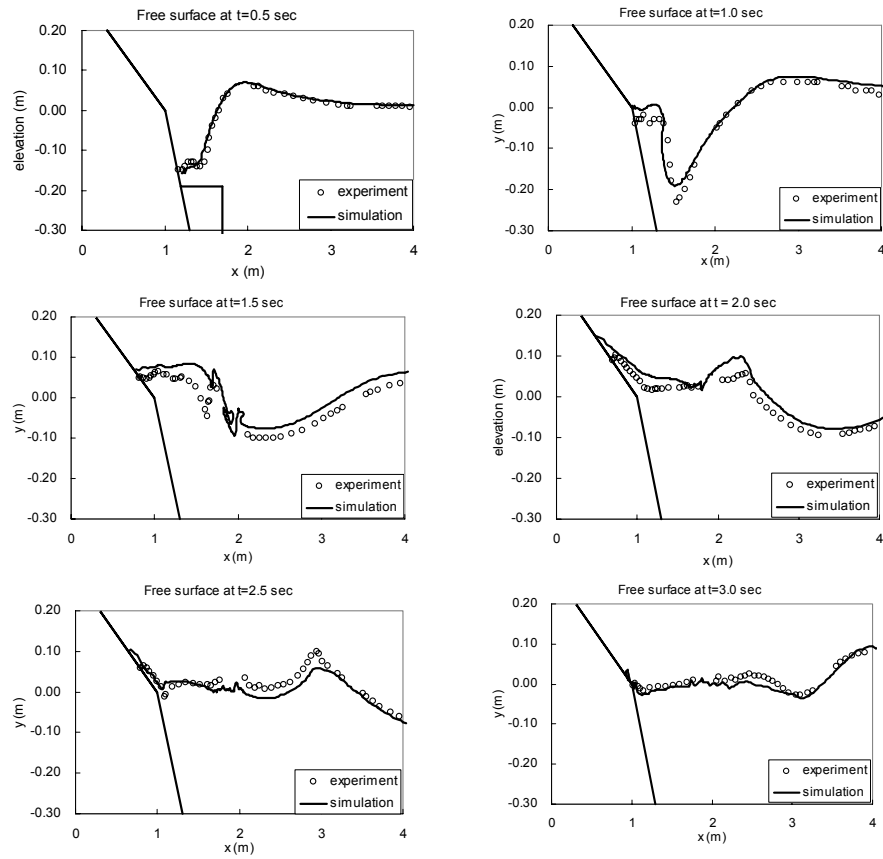


Fig 1. Free surface comparisons between simulation and experimental data at 0.5, 1.0, 1.5, 2.0, 2.5, and 3.0 s in wave generation region. First panel shows portion of triangular shape moving boundary.

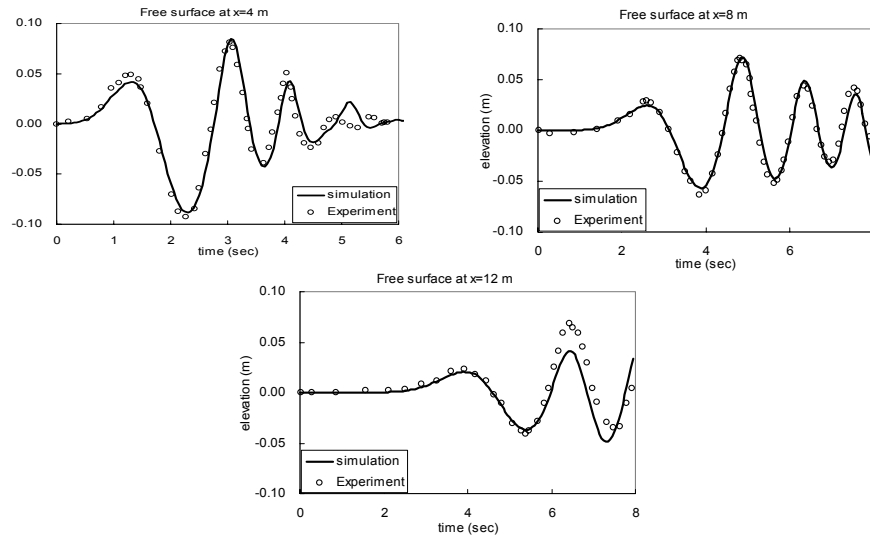


Fig 2. Free surface comparisons between simulation and experimental data at $x = 4, 8,$ and 12 m in propagation region.

A convergence test using minimum grid sizes of 0.005, 0.01, 0.02, and 0.04m has been performed. A fine grid of 30 cells is used to resolve maximum wave height. It is observed that convergence is achieved with a grid size 0.01m. This value (or smaller) is employed through out the study.

Turbulence generation by the submarine mass movement on a beach and its evolution are examined. Figure 3 shows the contours of turbulence intensity at $t = 0.5, 1.0, 1.5, 2.0, 2.5,$ and 3.0 seconds. It is observed that when the mass is in motion turbulence is generated around the upper right corner because of flow separation. Once the waves generated by the moving mass reach shore, waves are reflected. After the mass movement stops, turbulence is generated by the breaking of the reflected wave near the free surface and turbulence intensity decreases gradually. The maximum turbulence intensity can reach 0.83 m/sec, which is almost 50% of the mean velocity.

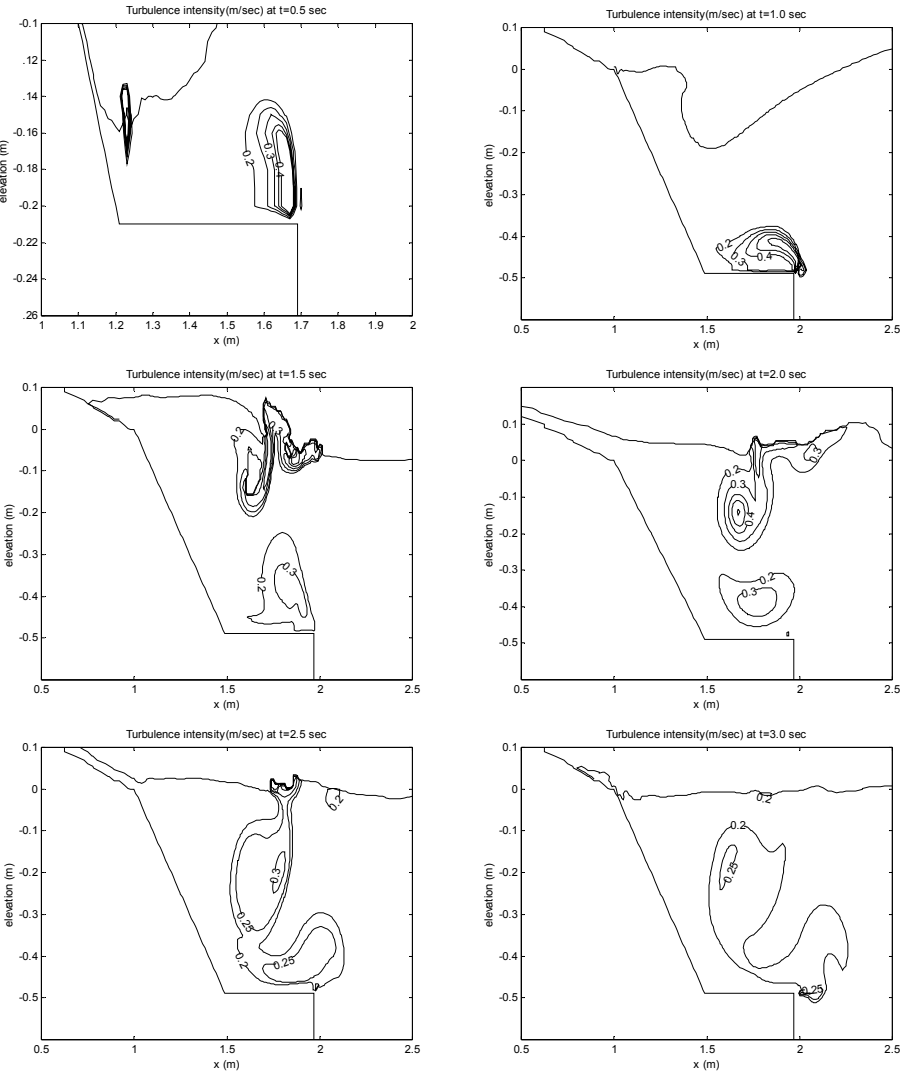


Fig 3. Turbulence intensity around moving body at $t = 0.5, 1.0, 1.5, 2.0, 2.5,$ and 3.0 seconds.

The influence of the submarine mass movement velocity is examined by varying the displacement time history. Denoting a_0 as the acceleration of the mass movement measured in the experiment, we have calculated three additional cases with accelerations that are $0.5a_0$, $0.75a_0$ and $1.25a_0$, respectively. In these simulations the total displacement and the volume of mass movement remain constant so that only one parameter, *i.e.*, velocity of the moving mass, is varied. The effects of mass movement velocity on maximum wave heights, runup and rundown are shown in Figures 3 and 4, respectively. As expected, the magnitudes of the wave height, runup and rundown increase with increasing acceleration, as shown in Figure 5.

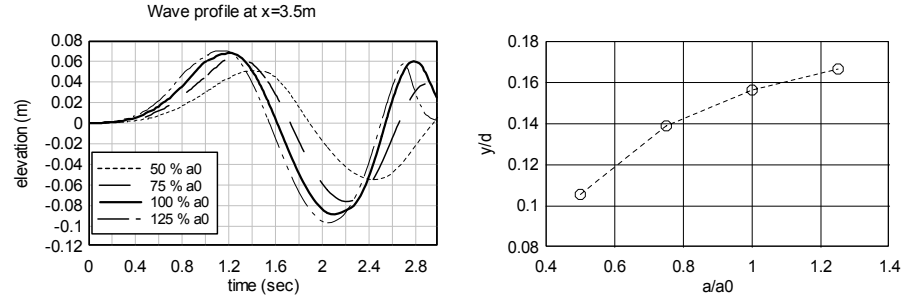


Fig 4. Influence of sliding mass velocity on wave height: (a) Time series of free surface at $x = 3.5$ m, (b) Maximum wave height.

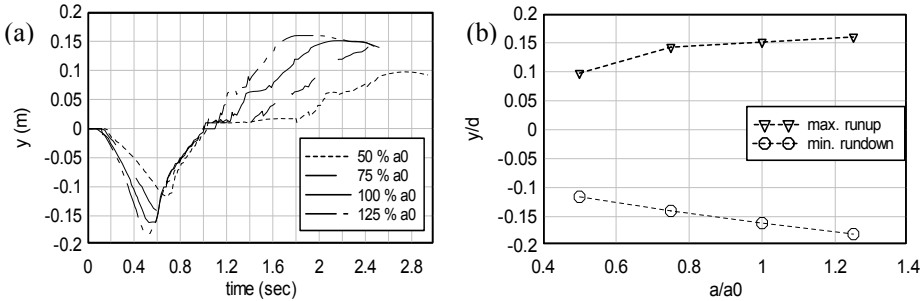


Fig 5. Influence of mass movement velocity on runup and rundown: (a) Elevation of free surface level along solid fixed boundary, (b) Maximum and minimum free surface level.

4 Concluding Remarks

The capability and accuracy of the present numerical model in predicting wave generation by submarine mass movement and propagation is validated. In addition, the influence of moving body velocity on runup and rundown is examined. For the higher sliding body velocity, maximum runup and rundown is increased as expected. In this study, sliding body motion is predetermined based on experimental data ahead of computation. However, in order to examine or predict the wave generation by the submarine mass movement without given velocity or displacement time history, it is necessary to consider the interaction between moving body and fluid in the future.

Turbulence generation by triangular shape moving body occurs around upper right corner due to flow separation and near the free surface where waves break. Careful

experiments measuring the velocity field are desirable to validate the prediction of the turbulence intensity.

5 Acknowledgements

Partial support from the National Science Foundation Grants CMS-9908392 and CMS-0217744, and the US Office of Naval Research Grants N00014-92-1221 and N00014-97-1-0581 are gratefully acknowledged.

References:

Grilli, S.T. and Watts, P. 1999 "Modeling of waves generated by a moving submerged body. Applications to underwater landslides". *Eng. Anal. Boundary. Elements*, **23**, 645-656.

Hammack, J.L. 1973. "A note on tsunamis: their generation and propagation in an ocean of uniform depth", *J. Fluid Mech.*, **60**, 769-799.

Heinrich, P. 1992. "Nonlinear water waves generated by submarine and aerial landslides", *J. Waterway, Port, Coastal and Ocean Engrg., ASCE*, **118**, 249-266.

Hsu, T.-J., Sakakiyama, T. and Liu, P.L.-F. 2002 "Validation of a model for wave-structure interactions". *Coastal Engrg*, **46**, 25-50.

Lin, P. and Liu, P.L.-F. 1998a "A numerical study of breaking waves in the surf zone". *J. Fluid Mech.*, **359**, 239-264.

Lin, P. and Liu, P.L.-F. 1998b "Turbulence transport, vorticity dynamics, and solute mixing under plunging breaking waves in surf zone." *J. Geophys. Res.*, **103**, 15677-15694.

Lin, P., Chang, K.-A., and Liu, P.L.-F. 1999 "Runup and rundown of solitary waves on sloping beaches". *J. Waterway, Port, Coastal and Ocean Engrg., ASCE*, **125** (5), 247-255.

Lynett, P.J. and Liu, P.L.-F. 2002 "A numerical study of submerged landslide generated waves and runup", *Proc. Royal Soc. A*. **458**, 2885-2910.